

Life in the Slow Lane: A Search for Long Term Variability in ASAS-SN

Sydney Petz,¹* C. S. Kochanek,^{1,2}

¹*Department of Astronomy, The Ohio State University, 140 W 18th Avenue, Columbus, OH 43210, USA*

²*Center for Cosmology and AstroParticle Physics, 191 W Woodruff Avenue, Columbus, OH 43210, USA*

Accepted XXX. Received YYY; in original form ZZZ

ABSTRACT

We search a sample of 9,361,613 isolated sources with $13 < g < 14.5$ mag for slowly varying sources. We select sources with brightness changes larger than ~ 0.03 mag/year over 10 years, removing false positives due to, for example, nearby bright stars or high proper motions. After a thorough visual inspection, we find 782 slowly varying systems. Of these systems, 433 are identified as variables for the first time and 349 are previously classified as variables. Previously classified systems were mostly identified as semi-regular variables (SR), slow irregular variables (L), spotted stars (ROT), or unknown (MISC or VAR), as long time scale variability does not fit into a standard class. The stellar sources are scattered across the CMD and can be placed into 5 groups that exhibit distinct behaviors. The largest groups are very red subgiants and lower main sequence stars. There are also a small number of AGN. There are 551 candidates (~ 70 percent) that also show shorter time scale periodic variability, mostly with periods longer than 10 days. The variability of 191 of these candidates may be related to dust.

Key words: surveys – stars:variables: general

1 INTRODUCTION

There are an increasing number of time domain surveys such as the All-Sky Automated Survey for SuperNovae (ASAS-SN; Shappee et al. 2014; Kochanek et al. 2017; Jayasinghe et al. 2018), the Zwicky Transient Facility (ZTF; Bellm 2014), the Asteroid Terrestrial-impact Last Alert System (ATLAS; Heinze et al. 2018) and soon the Legacy Survey of Space and Time at the Vera Rubin Observatory (LSST; Hambleton et al. 2023). These surveys are largely focused on the transient universe and variable stars, usually only considering long term variability when looking at active galactic nuclei (AGN). These surveys (as well as earlier surveys) have never systematically explored the slowly varying universe. Known classes of longer term variability include magnetic activity cycles on main sequence stars Baliunas & Jastrow (1990), active K giants (Phillips & Hartmann 1978), and some classes of young stellar objects (YSOs, Teixeira et al. 2018). There are also rarer types including stellar mergers (Tylenda et al. 2011) and peculiar stellar dimmings (Simon et al. 2018).

Some of the first explorations of slow variability used sporadic measurements of solar-type stars over several decades (Baliunas & Jastrow 1990). Much like our Sun, they showed cyclic variations in brightness that correspond to magnetic activity cycles. Magnetic activity and its relation to variability has also been studied in M dwarfs, finding links between brief dips and increases in brightness, rotational spot modulation, and flaring activity (Weis 1994). There are cyclic variations on year timescales and a correlation between stronger photometric fluctuations and position above the main sequence (Hosey et al. 2015; Clements et al. 2017).

Slow variability has also been observed in K giants on longer

timescales. Proposed explanations include obscuration from ejected dust shells, lithium flashes, or unstable helium shell burning as these stars begin to ascend up the AGB (Tang et al. 2010). The irregular brightening and dimming of K giants may also have a magnetic component (Oláh et al. 2014), with changes in the spots and faculae accompanying changes in radius.

Though more traditionally known for their short-term variability, certain sub-classes of classical T Tauri stars (cTTS) exhibit long-term variability. These Type III cTTS vary by of tenths of a magnitude over a typical observing season due to large-scale variations in their accretion rates or the circumstellar disk region partially occulting the central star (Grankin et al. 2007). These stars can also exhibit smooth changes in mean brightness on timescales of years.

Stellar mergers (also called luminous red novae) are rare, with an estimated rate of approximately one per year in the Galaxy (Kochanek et al. 2014). After the "classical" transient associated with their peak luminosity, they are observed to slowly evolve for decades. Interestingly, some systems including V1309 Scorpii and M31-LRN-2015 were observed to show steady variability changes years before their mergers (Tylenda et al. 2011; Blagorodnova et al. 2020), and there are theoretical reasons to expect that all of these systems do so (Metzger & Pejcha 2017; Matsumoto & Metzger 2022). This has led to attempts to identify systems which might be in this pre-merger phase (e.g., Molnar et al. 2017; Addison et al. 2022).

There are several examples of slow variability that have yet to be fully explained. One example is the main sequence F star KIC 8462852, which has exhibited an unusual series of brief dimming events resulting in a cumulative fading of 3 percent (Montet & Simon 2016). Although the individual dimming events could be attributed to polar spots over a period of years or transiting circumstellar material, the long-term variability is not well explained. A more dramatic example is the cool giant Gaia17bpp which exhibited ~ 4.5 magni-

* E-mail: petz.16@osu.edu

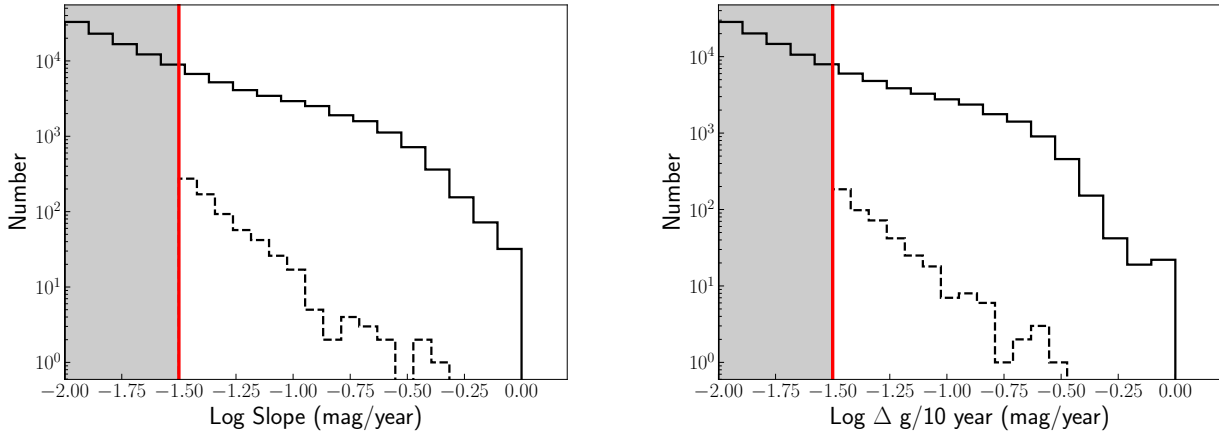


Figure 1. Distributions of the input sources (solid) in linear slope (left) and maximum magnitude change Δg in the quadratic fit (right). We considered sources to the right of the red lines with slopes or $\Delta g/10 \text{ year} > 0.03 \text{ mag/year}$. The dashed histograms show the distributions of the final sample after eliminating false positives.

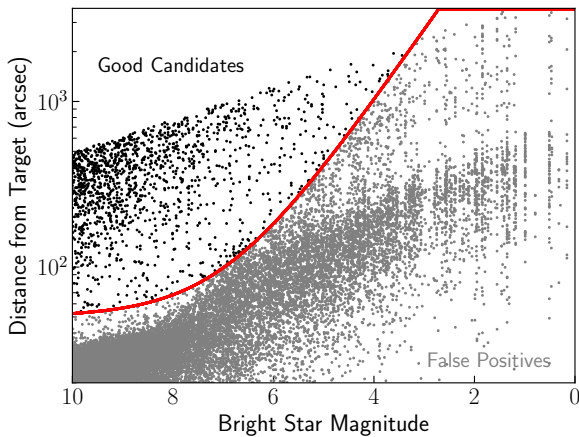


Figure 2. Distribution of the initial candidates in the magnitude and distance of bright nearby stars. We keep stars above the red curve.

tude dimming event over a period of more than 6.5 years (Tzanidakis et al. 2023). Though not the only dimming event observed over such a long interval (e.g., Rowan et al. 2021; Smith et al. 2021; Torres & Sakano 2022), it is one of the deepest and longest known events. Although proposed to be a binary star system with a secondary star enshrouded by an optically thick debris disk (Tzanidakis et al. 2023), the nature of this system is not fully understood, as the secondary star has yet to be identified. A main-sequence F star, known as Boyajian’s star (Boyajian et al. 2016), has exhibited unusual brightening episodes followed by a steady dimming since 2013 (Simon et al. 2018). Multiple theories for these events have been suggested, including the ingestion of a planet and its satellite system (Metzger et al. 2017) and energy from the convective structure of the star (Foukal 2017). Another interestingly varying source is KH 15D, a pre-main sequence star with a history of variation that dates back 60 years. This weakly accreting T Tauri binary has exhibited photometric variations likely linked to a precessing circumbinary disk and scattered light (Herbst et al. 2010). The rise and fall of Sakurai’s

object (V4334 Sgr) marks another dramatic example of slow variation, with a helium flash causing a several magnitude increase in brightness followed by an approximately 11 magnitude decline over several years due to growing dust obscuration (Duerbeck et al. 2000).

Using 11 years of monitoring data, Neustadt et al. (2021) observed 26 nearby galaxies with the Large Binocular Telescope (Kochanek et al. 2008; Gerke et al. 2015) to search for failed supernovae. During this search, they identified a peculiar population of luminous stars slowly changing in brightness by factors of ~ 3 at nearly constant color. These stars were too faint to easily characterize, but we can potentially identify Galactic analogues. With approximately 10 years of observations, ASAS-SN has obtained photometric measurements of ~ 100 million stars with $g \lesssim 18.5 \text{ mag}$. Here we use the ASAS-SN data to search for slowly varying sources. We describe the methods in §2 and the results in §3. We discuss possible follow up studies and survey extensions in §4.

2 METHODOLOGY

We first downloaded the light curves of the 9,361,613 sources with $13 < g < 14.5 \text{ mag}$ from ASAS-SN Sky Patrol V2.0 (Hart et al. 2023). We then intercalibrated the cameras and both the V and g band data using a damped random walk Gaussian process for interpolation with the camera/filter calibration shifts fit as additional linear parameters (see Kozłowski et al. 2010). Next, we computed seasonal medians to eliminate all short time scale variability. We use the median rather than the mean as it is insensitive to outliers. We then fit the seasonal medians using both a linear and a quadratic function of time. Fig 1 shows the distribution of linear slopes. We kept candidates with linear slopes greater than 0.03 mag/year . We used the quadratic fits to estimate the maximum implied difference in magnitude Δg over the length of each light curve. We kept stars with a Δg greater than 0.3 magnitudes. With roughly $\Delta t \approx 10$ years of data, a $\Delta g > 0.3 \text{ mag}$ implies a "slope" $\Delta g / \Delta t \gtrsim 0.03 \text{ mag/year}$, as also shown in Fig 1. This left us with 36,705 candidates.

Among the initial candidates, we find four classes of false positives. The first class is a range of artifacts created by bright stars. Because of the bleed trails of saturated stars, the star causing the false positives can be quite distant. Figure 2 shows all the initial candidates with

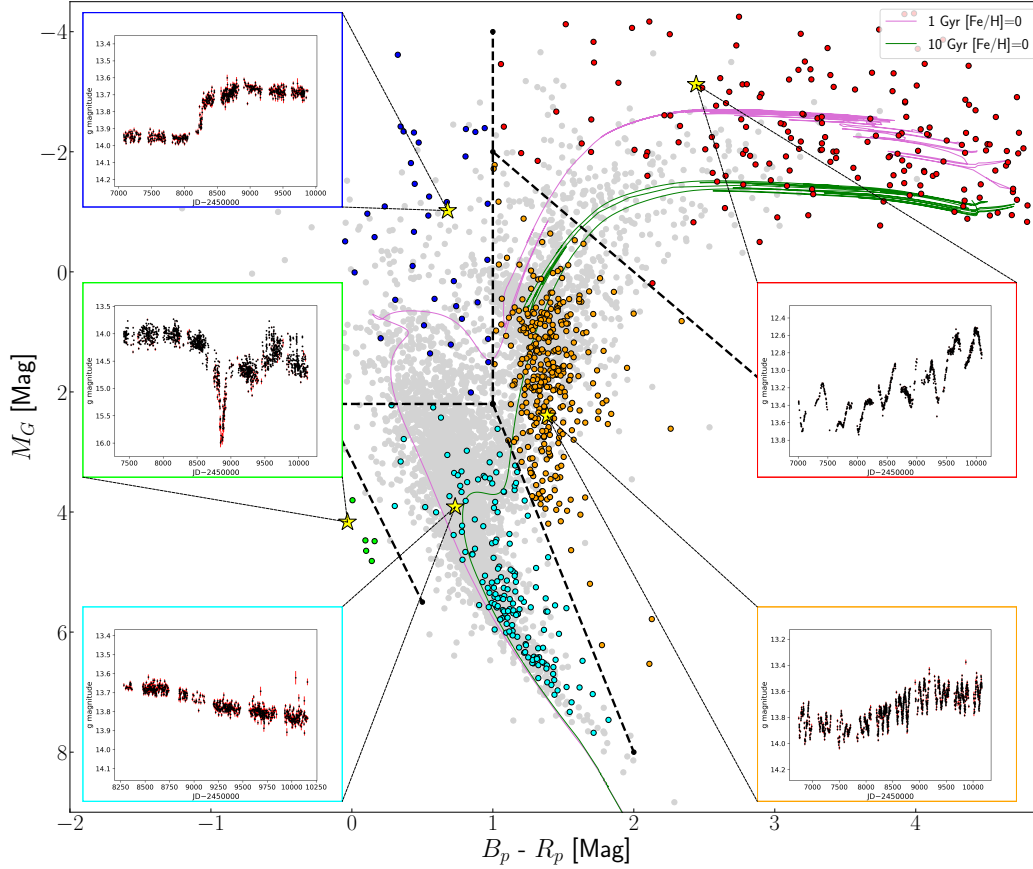


Figure 3. The Gaia DR3 M_G and $B_P - R_P$ color-magnitude diagram of the final candidates divided into groups based on the dashed lines. The curves are solar metallicity 1 and 10 Gyr MIST isochrones. One type of light curve is shown in each group.

absolute linear slopes greater than 0.03 mag/year in the space of the distance and magnitude of nearby bright stars. We identify two bands, with the lower band consisting of false positives due to the nearby bright stars. To discard these false positives, we keep the stars above the quadratic curve shown in Figure 2 up to a maximum distance of 3600 arcseconds at brighter magnitudes. This reduces our sample to 6690 stars.

The second class of false positives is stars near the celestial south pole. Due to field rotations created on ASAS-SN’s equatorial mounts, there is a concentration of stars with nonphysical maximum magnitude differences at this pole. To account for these, we discard any candidates with declinations less than -88 degrees. This cuts 75 additional stars from our sample.

The third class of false positives are high proper motion stars or stars near high proper motion stars. While ASAS-SN photometric apertures are fairly large (radius of $16''$), stars with sufficiently large proper motions will create a signal as they move through the aperture. Because the resolution is low, sufficiently bright non-target stars moving through the aperture will also create a signal. To remove these objects from our sample, we discard stars with proper motions higher

than 100 mas/year or where a nearby star with a flux ratio greater than 0.01 passes through the photometric aperture. This removes 49 of the remaining candidates.

We examined the remaining light curves and their corresponding ASAS-SN images individually. In doing so, we can not only begin to examine the long-term trends of these objects but also remove targets that appear too noisy or are still being affected by nearby bright stars. During this process, we discovered a fourth source of false positives, stars with insufficient overlap between the V and g band data where the intercalibration process fails. This sometimes leads to a magnitude jump, mimicking a brightening event. We discard these targets as a part of our visual inspection. This left us with the 782 candidates listed in Table 1. Their distribution in slope and Δg is shown in Fig. 1. One useful initial check for systematic problems is that there are roughly equal numbers of sources becoming brighter (395) and fainter (387), so they are not affected by systematic drifts in the photometry.

We cross matched these sources with Gaia Alerts (Hodgkin et al. 2021), and the AAVSO VSX catalog (Watson et al. 2006), which contains variables identified by amateurs and surveys such as ASAS-SN

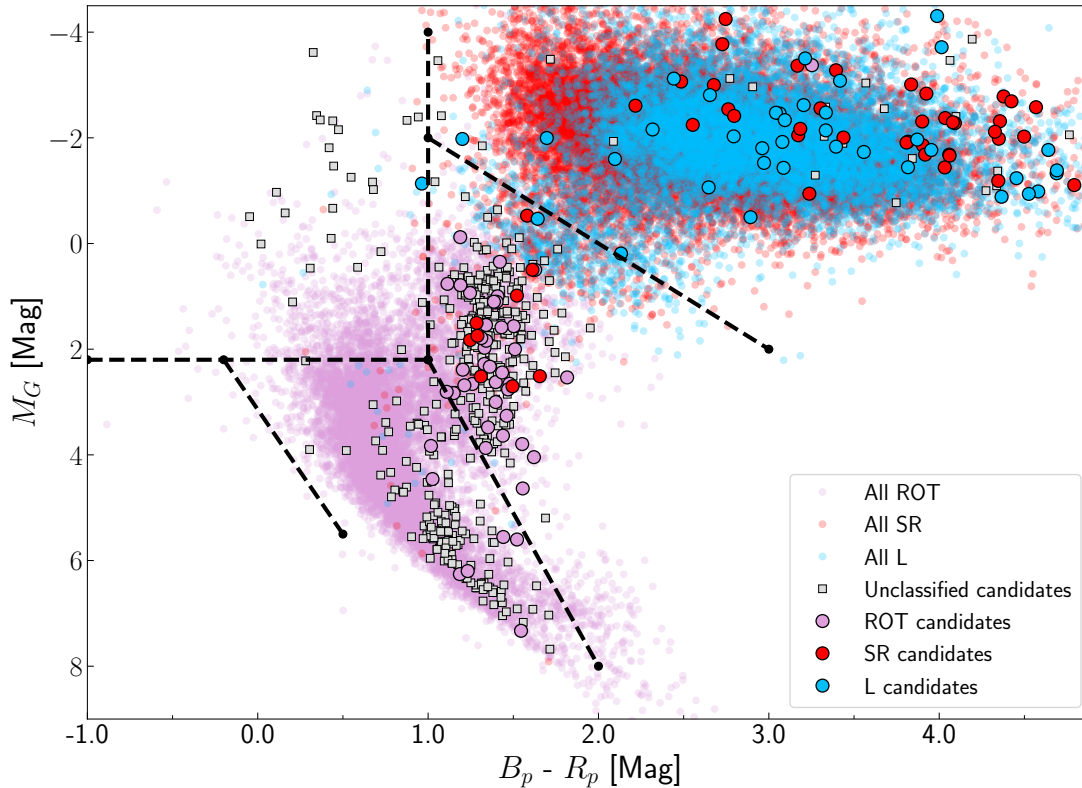


Figure 4. The Gaia DR3 M_G and $B_P - R_P$ color-magnitude diagram of all variables in SkyPatrol V2.0 with $13 < g < 14.5$ that are classified as SR, L, and ROT (small points) as compared to the candidates with these classifications (large points). Previously unclassified candidates are marked by squares.

(Jayasinghe et al. 2020, 2021; Christy et al. 2023), ATLAS (Heinze et al. 2018), WISE (Chen et al. 2018), and ZTF (Chen et al. 2020). We match our final candidates with Gaia DR3 photometry (Gaia Collaboration et al. 2023), use distances from Bailer-Jones (2023), and correct for extinction with `mw dust` (Bovy et al. 2016), which is based on the dust maps of Drimmel et al. (2003), Marshall et al. (2006) and Green et al. (2019). We identified likely active galactic nuclei (AGN) by matching the sources to the `milliquas v8` catalog (Flesch 2023). We used SIMBAD (Wenger et al. 2000) to obtain general stellar classifications and spectral types if they were available. Because many of the candidates appear to be periodic on shorter time scales, we fit and subtract a linear or quadratic trend from each light curve to remove the observed long time scale trend and then use a Lomb-Scargle periodogram (Lomb 1976; Scargle 1982) to search for periodicity. We discard periods longer than the average observing season and kept the most significant period with a false alarm probability < 0.1 for each candidate to remove nonphysical periods. We also extract Near-Earth Object Wide-field Infrared Survey Explorer (NEOWISE; Mainzer et al. 2014) infrared light curves for each source using Hwang & Zakamska (2020). We combine closely spaced points, and fit the W1 light curve and the W1–W2 color evolution with linear and a quadratic functions of time.

3 RESULTS

After searching through a sample of 9,361,613 objects within $13 < g < 14.5$ magnitudes, we find a total of 782 candidates exhibiting long term variability. This includes 349 objects previously flagged as variables, and 433 new variables. We show all of the candidates in Fig. 3 on a Gaia DR3 M_G and $B_P - R_P$ color magnitude diagram as well as Solar metallicity 1 Gyr and 10 Gyr MIST (Paxton et al. 2018) isochrones to track stellar evolutionary stages. We loosely separate the stellar candidates into five main groups based on the isochrones in Fig. 3: main sequence, subgiant/giants, AGB stars, luminous blue stars, and novae. We find that the variables in each group usually exhibit different physical characteristics in their light curves. Due to negative or missing parallaxes and distances in Gaia DR3 (Gaia Collaboration et al. 2023) and Bailer-Jones (2023), 27 candidates cannot be placed into a group, and 4 of these are AGN.

The two most common types of known variables in the sample are semi-regular (SR) and slow irregular (L) pulsating variables, with a total of 112 pulsating variables in all. There are also 88 classified as a variable of unknown type (MISC or VAR), which is not surprising since the slow variability we are searching for is not a standard type. There are also 13 eclipsing variables, 53 rotating variables, 41 eruptive variables and 13 cataclysmic variables. Three were assigned to multiple types and 8 were identified as AGN in `milliquas v8`. Fig. 4 compares the candidates previously classified as SR, L, and ROT candidates to all such variables in SkyPatrol v2.0

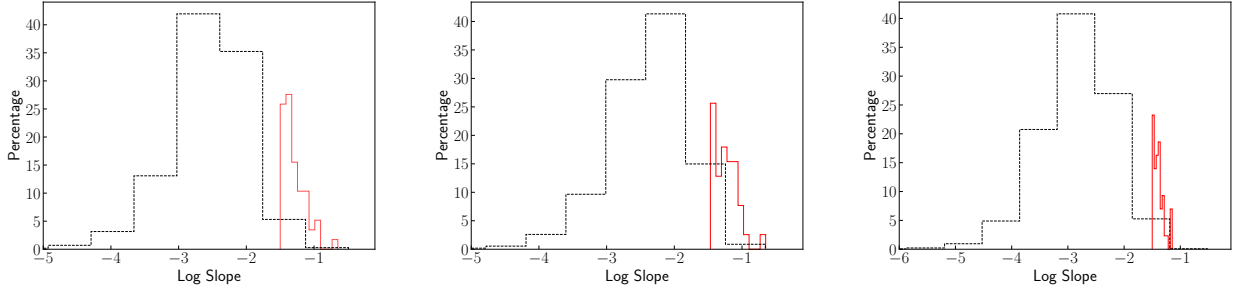


Figure 5. Slope distribution of the candidates (red solid) and all variables (black dashed) in SkyPatrol V2.0 with $13 < g < 14.5$ that are classified as SR (left), L (middle), and ROT (right).

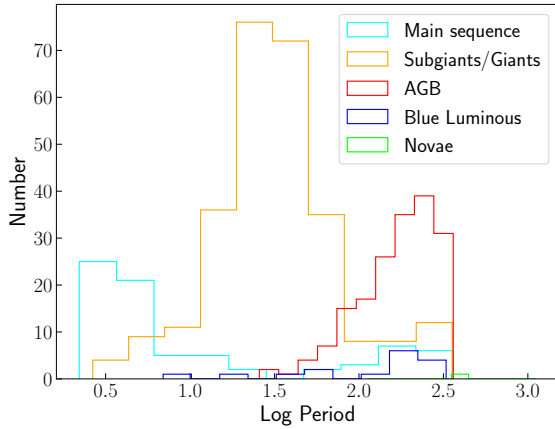


Figure 6. Period distribution for the candidates by group.

with $13 < g < 14.5$ mag in a Gaia DR3 M_G and $B_P - R_P$ color magnitude diagram and Fig. 5 compares their slope distributions. The candidates previously classified as ROT variables are RS CVn or subgiant rotational variables while many of the new systems are on the main sequence. Many of the candidates previously classified as SR variables also appear to be these rapidly rotating (sub)sub-giant stars. The remaining candidates previously classified as SR variables and those classified as L variables appear somewhat more luminous than the typical systems.

Fig. 6 shows the distribution of the periodic variables in each group, and Fig. 7 shows two examples with a roughly sinusoidal periodic signal on time scales short compared to the long term trends (40 days for the one from the giant/subgiant group, and 3.8 days for the main sequence example). Not surprisingly, the periods are basically just ordered by stellar size, with the main sequence group at short periods, the subgiant/giants at intermediate periods, and the AGB group at long periods. There are few periodic stars in the luminous blue and nova groups. Fig. 8 compares the rotation periods of our candidates previously classified as SR, L or ROT variables to all such variables with $13 < g < 14.5$ in SkyPatrol V2.0.

An important question is the extent to which the optical variability is associated with dust. Fig. 9 shows two comparisons of the optical and WISE mid-IR properties of the candidates. The right panel compares the optical extinction corrected $B_P - R_P$ color to the mean WISE $[W1] - [W2]$ color. We exclude stars with $[W1] < 9$ mag

where saturation starts to affect the colors. In this space, stars redder than $[W1] - [W2] \sim 0.3$ mag are good candidates for stars with circumstellar dust because they have a significant mid-IR excess. The left panel compares the optical G-band light curve slope s_G and the mid-IR $[W1] - [W2]$ color s_{col} . Candidates for variability driven by new dust formation should have $s_G > 0.03$ (fading) and $s_{col} > 0.004$ (becoming redder), while variability driven by dust being destroyed or becoming more distant from the star should have the reverse. We flag 171 fading/brightening systems and 20 systems with a mid-IR excess as possible dust driven variability candidates, as shown in both panels in Fig. 9. Fig. 10 shows examples of (1) a clear dust event, (2) a Be star in the SMC (Heydari-Malayeri 1990) with a mid-IR excess but no evidence that dust drives the changes in the optical brightness, and (3) V919 Sgr, which shows large optical variability and little mid-IR response. V919 Sgr is a symbiotic variable (Iverson et al. 1993), so the large amplitude g-band variability is likely driven by variable accretion onto the white dwarf companion of the cool giant.

There are 169 candidates in the main sequence group, of which 76 show additional periodicity. Their mean brightness changes are fairly linear, with modest bumps and wiggles. They are concentrated towards the lower main sequence in the CMD (Fig. 3), with periods generally greater than ~ 3 days when periodic. They appear to largely lie below the Kraft break (Kraft 1967), which suggests that rotation, convection and magnetic activity are driving the variability. Roughly, 10 percent of the sources are listed as YSOs (11) or T Tauri stars (5) in SIMBAD (see Table 1). However, compared to all the ROT variables in this magnitude range, there are many fewer short period systems, as seen in Fig. 8. The slope amplitudes appear to simply correspond to the high amplitude tail of the distribution for rotational variables in Fig. 5. Their behavior does not seem to be associated with dust since only a few have red mid-IR colors or significantly opposite signs for the slopes of the optical flux and the mid-IR color. Fig. 11 shows six examples of light curves, where we select the three fading sources and three brightening sources with the minimum, median, and maximum amplitudes based on the larger of the slope and $\Delta g/10 \text{ years}^{-1}$. Additionally, we choose sources that have light curves that span at least 9 years. The typical example has a relatively steady trend extending over the decade of observation, but almost all show evidence of an extremum, which suggests that this is also roughly the timescale for starting to revert to the mean. There are stars with more abrupt shifts, such as the example in the top left panel, where the star maintains a roughly constant magnitude for the first 5 years and then fades by ~ 2 mag over the next 4 years.

The subgiant/giant group consists of 334 stars, nearly half of the final candidates. Stars in this group exhibit behavior similar to that of

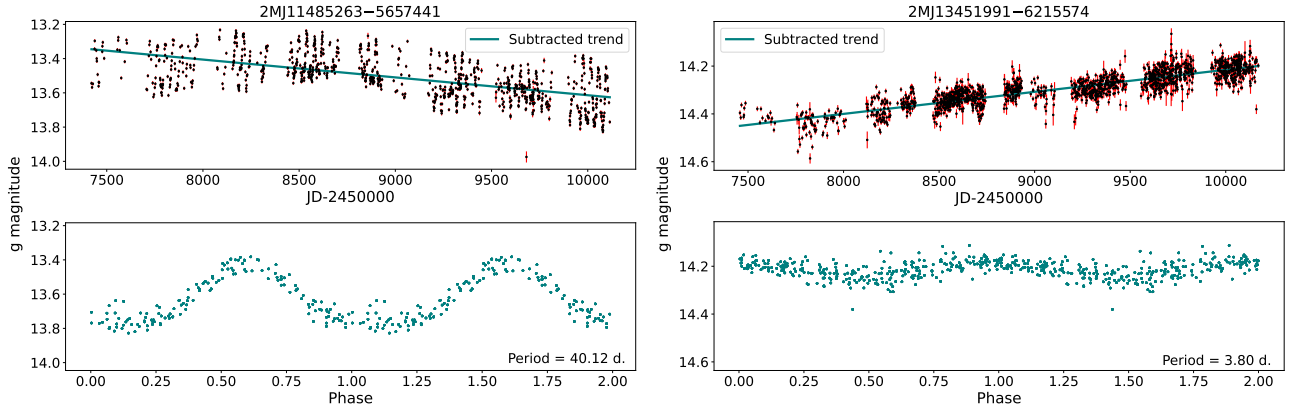


Figure 7. Phased light curves of two candidates displaying regular periodicity, labeled by their 2MASS ID. The top panel shows the light curve and the trend polynomial subtracted before estimating the period. The bottom panel shows the phased, detrended light curve. Left: A subgiant/giant group candidate with a period of 40.12 days. Right: A main sequence group candidate with a period of 3.80 days.

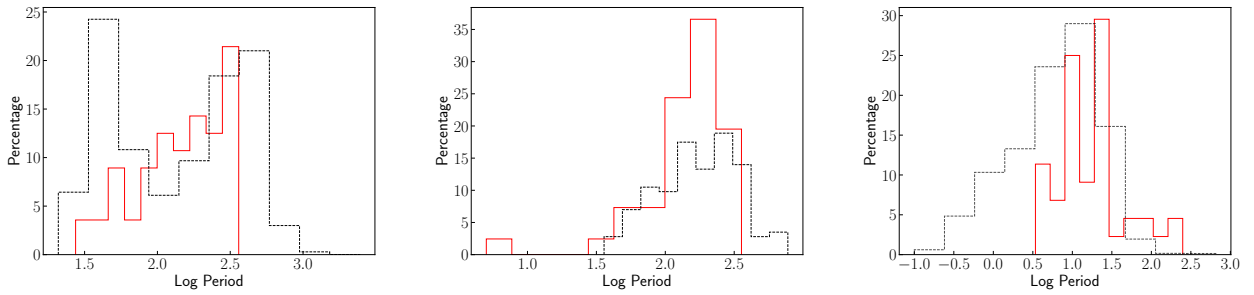


Figure 8. Period distribution of the candidates (red solid) and all variables (black dashed) in SkyPatrol V2.0 with $13 < g < 14.5$ that are classified as SR (left), L (middle), and ROT (right).

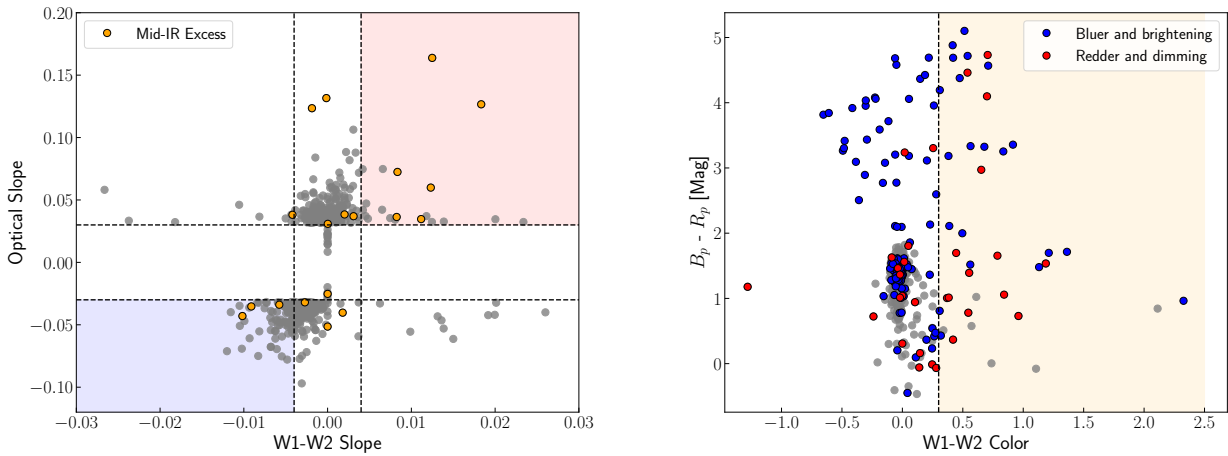


Figure 9. Left: Optical variability slope as a function of the W1–W2 color variability slope. Three stars are outside the edge of the figure, where 2 had bad WISE light curves and the third is the Nova V0339 Del (see Fig. 13). Red and blue shaded regions indicates candidates with W1–W2 > 0.3 mag that are likely getting redder and dimmer, or bluer and brighter. Right: $G_{BP} - G_{RP}$ color as a function of W1–W2 color. Candidates in the orange shaded region have a mid-IR excess due to dust emission. Candidates from the shaded region of each panel are shown with colored symbols on the other panel.

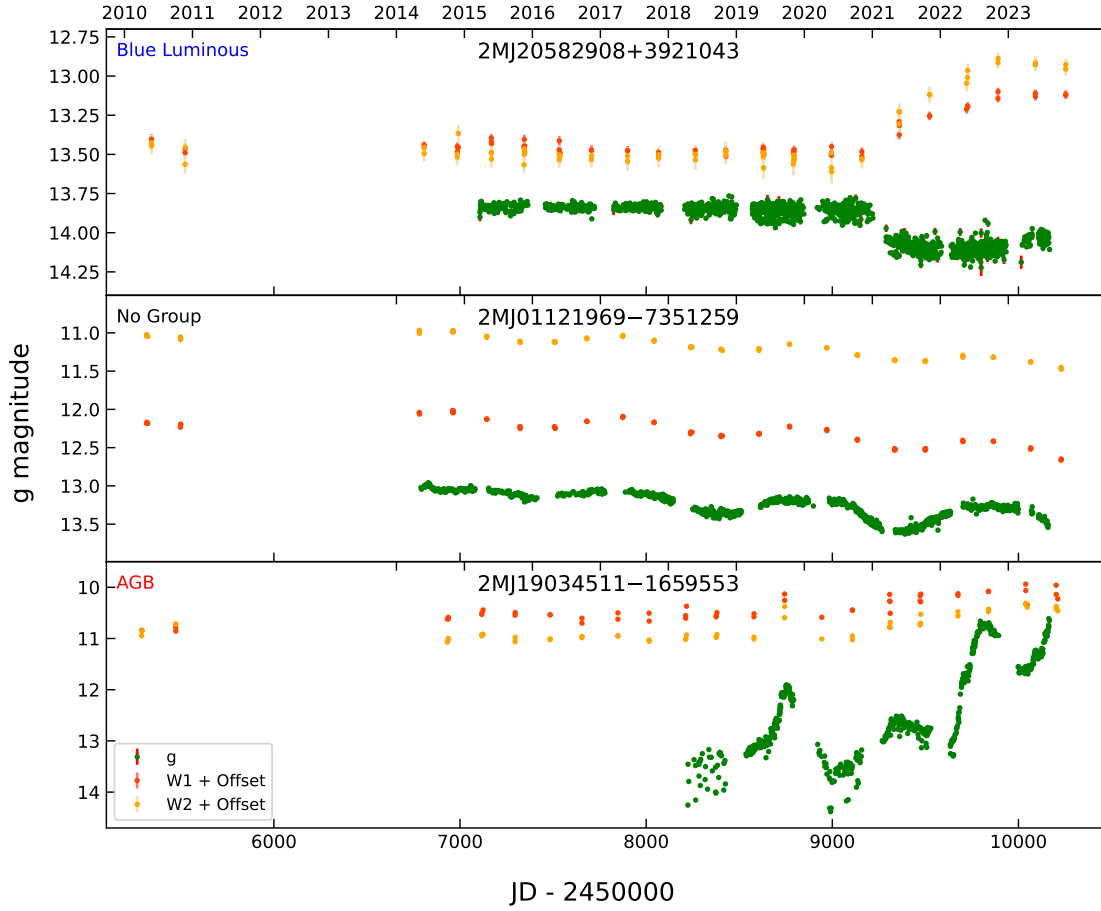


Figure 10. Comparisons of ASAS-SN and WISE light curves of candidates labeled by their 2MASS ID and CMD group. The top panel shows a candidate which clearly shows variability due to dust formation. The middle panel shows an example with very similar optical and mid-IR variability and a significant mid-IR excess. The bottom panel is the symbiotic star V919 Sgr, with a very large (~ 3 mag) optical brightening and a very small mid-IR brightening.

the main sequence group, typically having monotonically increasing and decreasing light curves. However, they tend to exhibit larger variability amplitudes in each season, and a larger fraction are periodic (273 of 334). The period distribution of the candidates is similar to that of the overall ROT/SR variables in this part of the CMD. In the Gaia CMDs, they lie towards the red edge of the $B_P - R_P$ color distribution both relative to all stars (Fig. 3) and stars classified as rotational variables (Fig. 4). They roughly lie in the region occupied by RS CVn and (sub)sub-giant rotational variables (see Phillips et al. 2024). Like the main sequence candidates, their amplitudes appear to simply be the extreme tail of the overall distribution (Fig. 5). 65 candidates are flagged for dust related variability. A few are classified in SIMBAD (see Table 1) as YSOs (3) and R CrB stars (1). Fig. 11 shows 6 example light curves. The typical example for this group generally has a steady trend over the decade of observation with shorter periodic variability. Like the main sequence group, many show evidence of an extremum. The top panels display examples of stars with more extreme shifts. The example in the top left has a steady trend over its first 4 years, followed by a dimming event of ~ 1 mag spanning several years and a period of slow brightening. The example in the top right slowly dims and brightens over 6 years

before abruptly brightening by 1 mag over a period of 2 years before again beginning to fade quickly.

The 203 candidates in the AGB group show distinct differences from the first two groups. They tend to have large amplitude variability within each season, and almost all show signs of periodicity (184 of 203). Their periodicity is generally SR-like, and their period distribution is similar to the overall variable population (Fig. 8). This group contains all 25 stars flagged in SIMBAD as Carbon stars (see Table 1). They are again simply the high amplitude tail of the slope distribution (Fig. 5). As noted earlier, they tend to be modestly more luminous than both randomly selected stars in that part of the CMD (Fig. 3) and known L/SR/ROT variables in that region (Fig. 4). Cross-matching these stars to SIMBAD, we find that 5 of them are cataloged as R Coronae Borealis variables (see Table 1). Three candidates from this group have a large mid-IR excess and one candidate classified as an R CrB star appears to have dust-related variability. Fig. 12 shows 6 example light curves, selected in the same way as for Fig. 11. The typical examples of this group have frequent, mostly irregular variability and slow brightness trends with amplitudes often larger than the first two groups and much longer periods. The examples with the largest overall long term variability are in the top panels. The top left

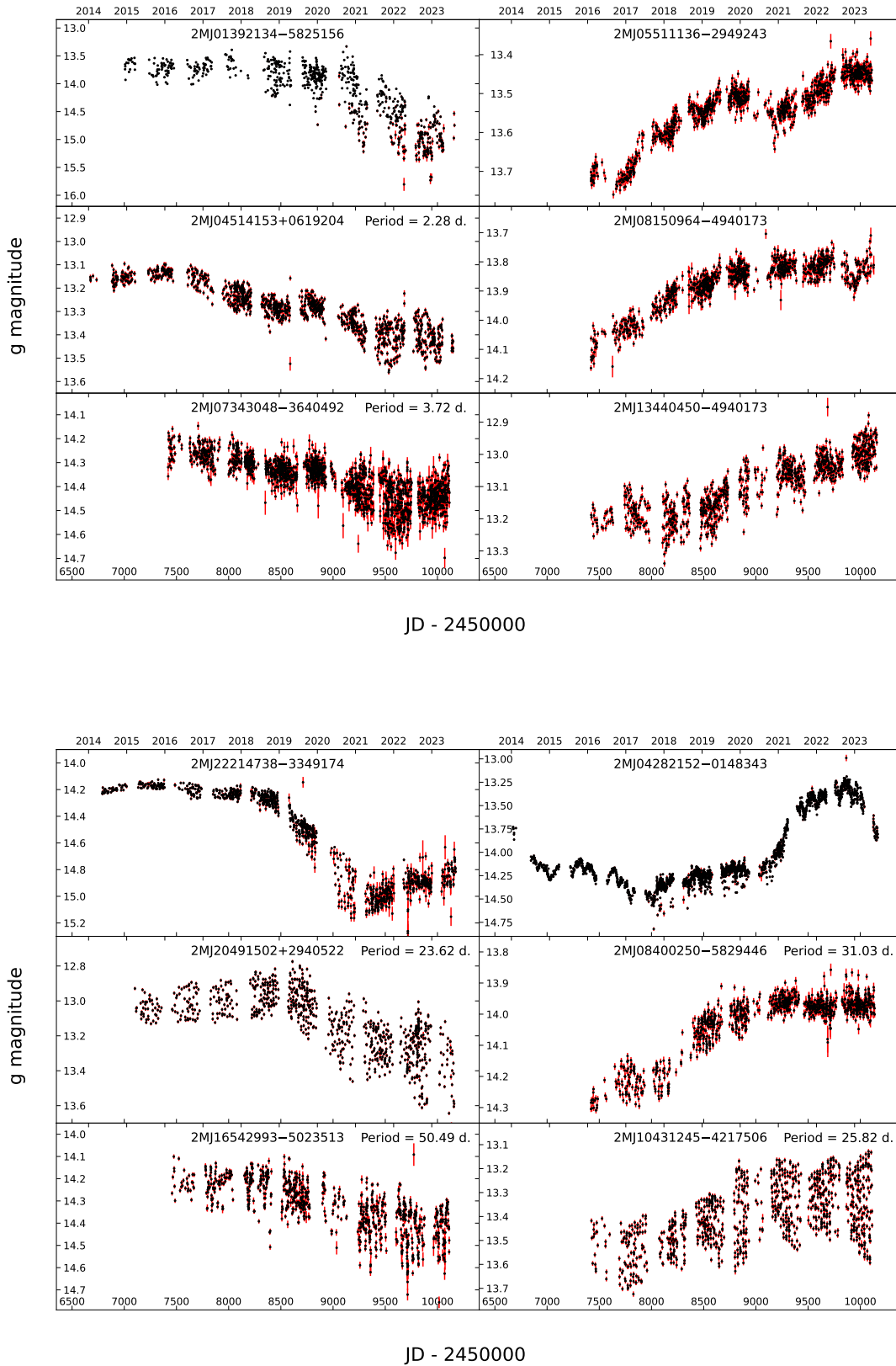


Figure 11. Example light curves for the main sequence group (top) and subgiant/giant group (bottom) labeled by their 2MASS ID. The left (right) panels show the 3 dimming (brightening) sources with the largest (top), median (middle), and smallest (bottom) slopes in the sample. The time axes are the same, but the magnitude ranges vary by object. If a period exists, it is given in the upper right corner.

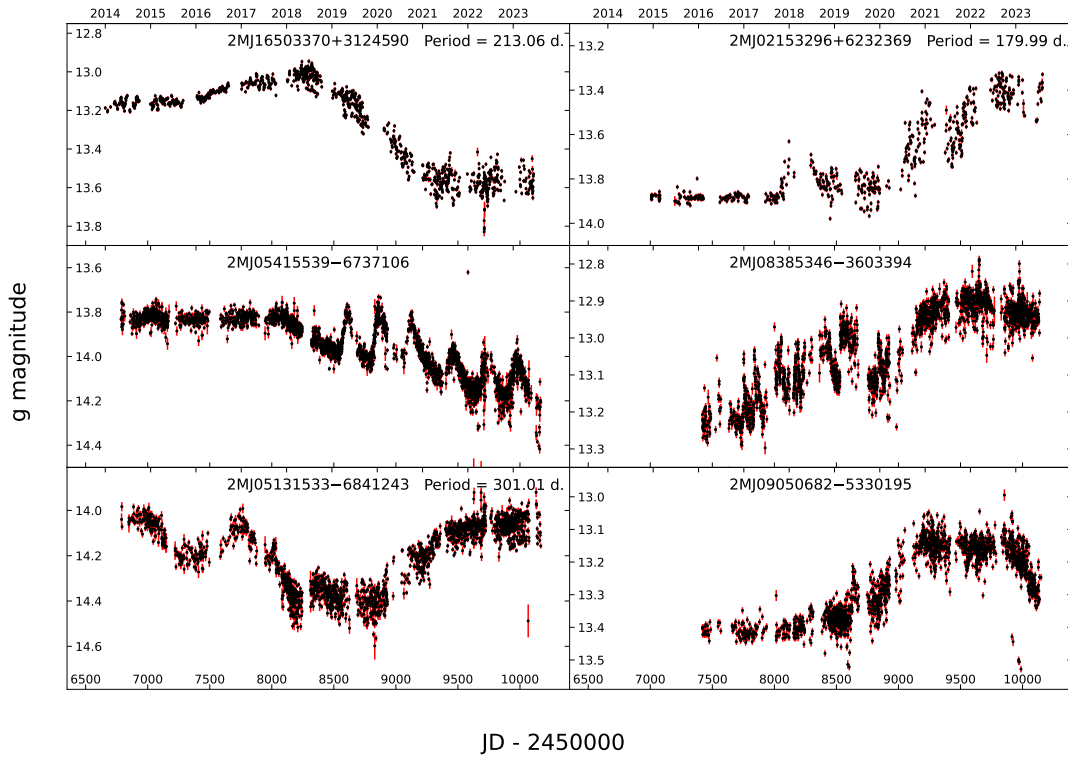
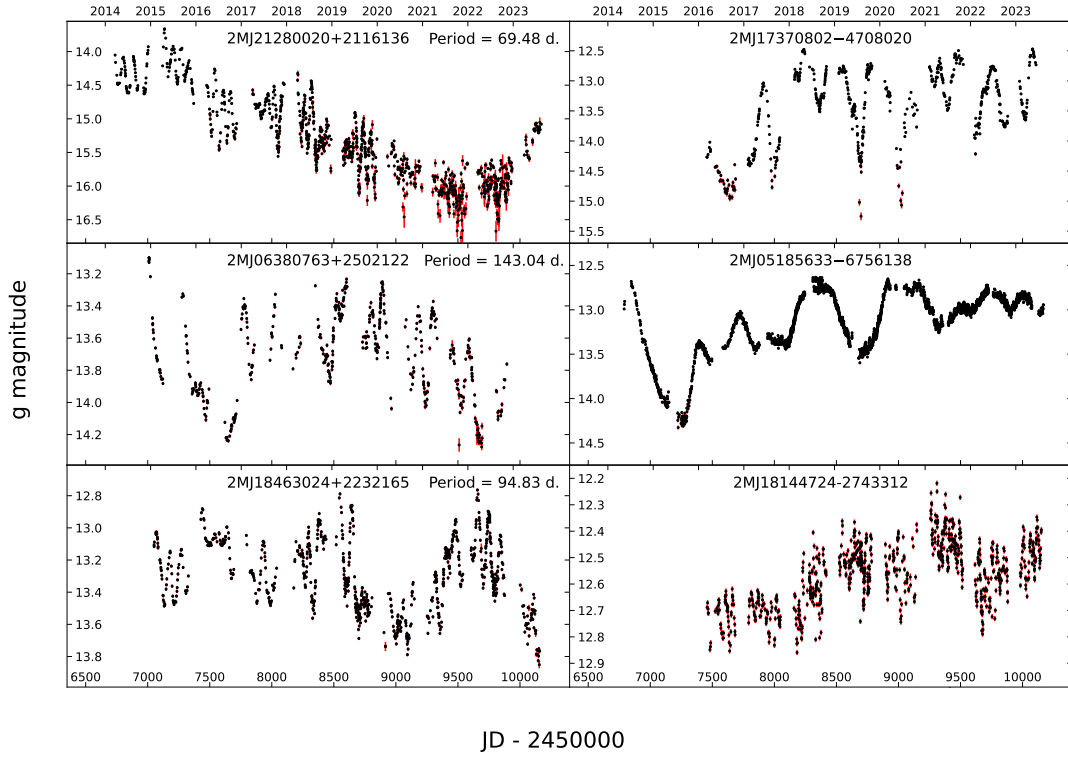


Figure 12. Example light curves for the AGB group (top) and luminous blue group (bottom). The format is the same as in Fig. 11.

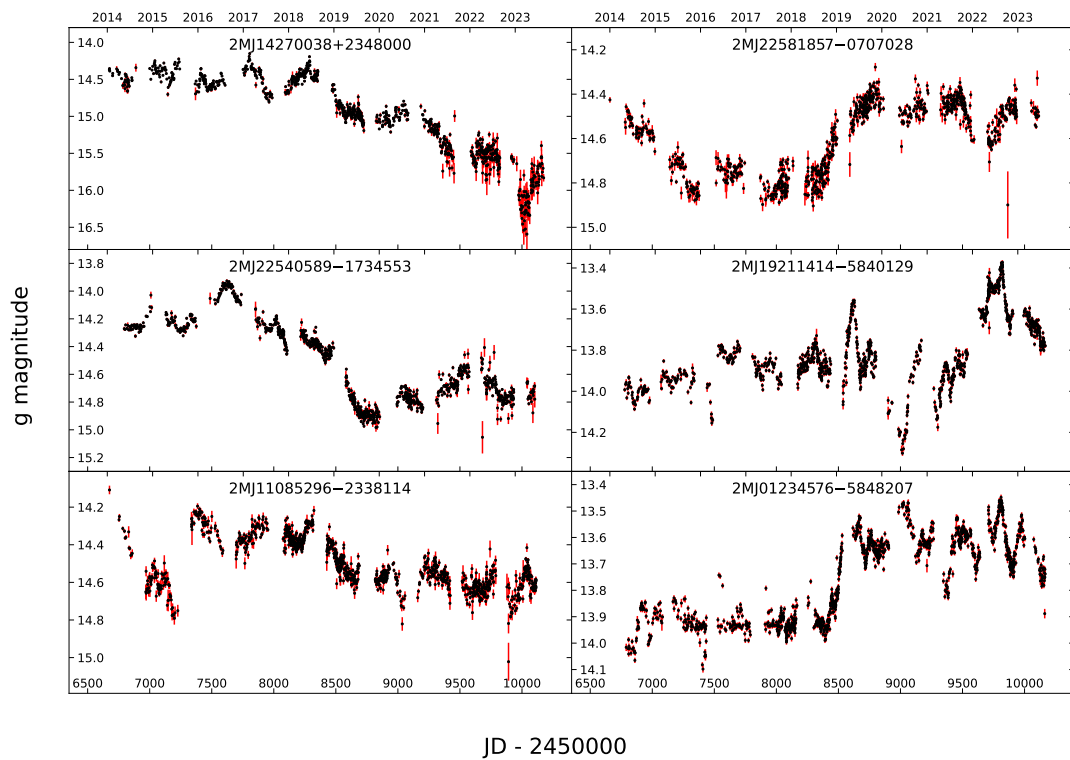
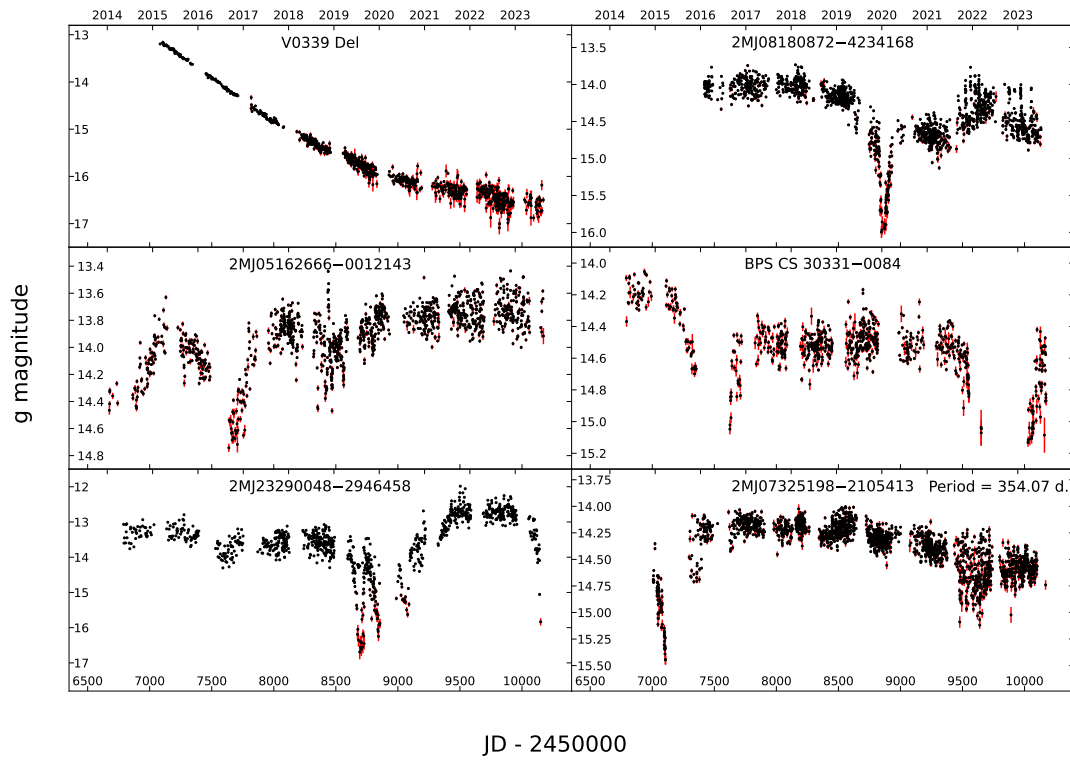


Figure 13. Example light curves for the novae group (top) and AGN (bottom). The source in the top left novae panel, V0339 Del, is simply a fading classical nova. The format is the same as in Fig. 11.

panel has a star with some periodicity that fades ~ 2.5 mag over 8 years before beginning to brighten. The top right panel contains a star with lots of short-term variability within its observing seasons, including multiple dimming events. In addition to these events, it increases its median brightness ~ 2 mag over the total duration of its light curve.

The blue luminous group is one of the smallest groups, containing, 43 candidates. This group mainly contains stars with sudden jumps or dips in their light curves, which are very different from the trends displayed in other groups. There are 17 periodic variables, but the remaining candidates generally are not periodic and exhibit the most stochastic behavior of the entire sample. Many of the candidates appear to have eruptive variability similar to the behavior of Be stars. We cross matched the stars with the Be Star Spectra Database (BeSS, [Neiner 2018](#)) and found only one match, but 7 are Be (1) or emission line (6) stars in SIMBAD (see Table 1). It was not obvious what existing variable class to use for comparisons of amplitudes and periods. Many of this group (18 out of 43 or ~ 42 percent) of this group were flagged as having dust driven variability such as the example in Fig. 10. Fig. 12 shows 6 example light curves, selected in the same way as for Fig. 11. Typical examples for this group contain more abrupt brightening or dimming events and show clear evidence of extrema, much like the first two groups. Their amplitudes of variability are sometimes more extreme, mirroring the amplitudes of the AGB group. The most extreme examples of variability in this group are shown in the top panels. The star in the top left panel maintains a relatively constant brightness for 4 years before rapidly fading and brightening over several years and then quickly dimming by ~ 3 mag. This dimming event lasts for ~ 1 year before the star begins to rapidly brighten once again.

The novae group sits to the left of the main sequence and contains only 6 candidates. This group is made up entirely of previously classified cataclysmic variables. One, nova V0339 Del ([Shore et al. 2013](#)), is a fading classical nova. The rest are “anti-dwarf” novae (NL/VY variables in AAVSO) showing short, deep dimming episodes. The fadings in the anti-dwarf novae are theorized to be caused by low rates of mass transfer from their luminous white dwarf companions ([Warner 1995](#); [Kato et al. 2002](#)). The amplitudes of this group appear to be larger than other CVs in AAVSO. Only one star from this sample had any periodicity, and two of the novae were flagged as having dust related variability. Fig. 13 shows all 6 as ordered in the earlier figures. Excluding V0339 Del, the typical behavior of this group is characterized by dimming events of various lengths.

We find that 8 of our final candidates are known AGN. These AGN have variability within each observing season and throughout the total duration of their light curves. Fig. 13 shows 6 example light curves.

The most dramatic brightness changes are seen in the top left panel, where the AGN PKS 1424+240 fades by ~ 2 mag over 10 years. PKS 1424+240 is a TeV-detected blazar ([Acero et al. 2015](#)) at a redshift of 0.60 ([Paiano et al. 2017](#)). 2MJ22581857–0707028 (RXSJ22583–0707) is a moderate ($z = 0.21$) redshift radio quasar, while the remaining 6 (2MJ0519–3239/ESO362–18, 2MJ0123–5848/ESO113–45, 2MJ1921–5840/ESO141–55, 2MJ0652+7425/IC450, 2MJ1108–2338/HE1106–2321, and 2MJ2254–1734/MR2251–178) all have $z < 0.1$.

4 CONCLUSIONS

We select 782 slow variable candidates out of a sample 9,361,613 sources with $13 < g < 14.5$ g mag. They were chosen to have mean

variability rates of ≥ 0.03 mag/year over roughly 10 years. This sample includes 349 previously classified variables and 433 new variables. However, the existing classifications do not capture this type of variability. We group these candidates into groups, finding that most are subgiants and giants. We find 551 candidates to be periodic, most having periods longer than 10 days and belonging to the subgiant/giant group. Using WISE light curves, we find 171 candidates with mid-IR brightness changes opposite to the optical, suggestive of changes in circumstellar dust and 20 candidates with a large mid-IR excess. The full list of variables is given in Table 1 and their light curves can be obtained using ASAS-SN SkyPatrol 2.0 (<http://asas-sn.ifa.hawaii.edu/skypatrol/>).

The main sequence candidates are below the [Kraft \(1967\)](#) break, they have the smallest slopes of the entire sample, and mostly have short periods if periodic. Only 20 are flagged as possibly having dust related variability. Their activity likely represents the extremes of star spot changes on longer time scales. Ten percent of these candidates are flagged as YSOs or T Tauri stars in SIMBAD. The subgiants/giants fall on the redder edge of the color distribution of RGB stars and ROT/SR variables, have similar amplitudes to the main sequence group, and have mostly intermediate length periods. Stars in this group are likely associated with RS CVn/(sub)sub-giant rotational variables. However, ~ 19 percent of these candidates are flagged as having dust-related variability. The flagged AGB stars seem to be slightly more luminous than L, SR, or random variables. Generally they have high amplitude slow (≥ 50 days) periodic variability as well. Only a few of these candidates (one is a R CrB variable) are linked to a large mid-IR excess, implying that their variability is not driven by dust.

The blue stars are more eruptive, with large amplitudes of variability and little periodicity. Their behavior seems similar to the behavior of Be stars, however only 7 are flagged as Be or emission line stars in BeSS and SIMBAD. A large fraction of this group is flagged as having dust related variability. The novae group has deep fadings spanning several magnitudes and is entirely made up of cataclysmic variables. Finally, we find a small number of AGN (8), where the highest amplitude source is the $z=0.60$ blazar, PKS 1424+240.

Particularly for the systems with the largest optical flux changes, it would be interesting to compare the spectra and spectral energy distributions of the stars in their high and low states. For cool stars, large changes at V-band can be driven by modest changes in temperature without similarly large changes in luminosity, but this is more challenging for the high amplitude blue stars where the g-band no longer lies on the blue wing of the spectral energy distribution. We plan to expand our list of candidates by continuing the search for slow variability in both brighter saturated stars (see [Winecki & Kochanek 2024](#)) and dimmer than our current magnitude range. As the time spanned by ASAS-SN continues to grow, we plan to search for smaller variations and explore lower amplitudes of variability. Searches for still slower changes than ~ 0.03 mag/year will require significant improvements in false positive rejection and/or longer light curves.

ACKNOWLEDGEMENTS

CSK is funded by NSF grants AST-2307385 and AST-2407206. We acknowledge ESA Gaia, DPAC and the Photometric Science Alerts Team (<http://gsaweb.ast.cam.ac.uk/alerts>) This research has made use of the SIMBAD database, operated at CDS, Strasbourg, France We acknowledge with thanks the variable star observations from the AAVSO International Database contributed by observers

Table 1. Long-term variability candidates and their properties. The full table is available in the electronic version of the paper. The classifications and spectral types are from SIMBAD.

2MASS	<i>g</i>	Optical Slope (mag/yr)	Δg	Group	Period (days)	W1–W2 Color	W1–W2 Slope	Classification	Spectral Type
2MJ13390896–0318071	13.00	0.041	0.373	Subgiant/giant	19.704	–0.056	0.001
2MJ20324096+4114291	13.02	0.035	0.282	AGB	33.905	0.700	0.012	...	B3–4Ia+
2MJ18035783–2425349	13.03	–0.088	0.756	...	199.814	0.562	–0.020	...	K0
2MJ08371244–2846184	13.03	0.066	0.516	Blue Luminous	60.243	–0.409	–0.028
2MJ18172030–4756384	13.04	–0.071	0.769	Main Sequence	4.461	–0.023	–0.012	EB	...
2MJ09243724–2804347	13.04	–0.043	0.383	Subgiant/giant	...	–0.046	–0.004	SB	...
2MJ19491489+4221569	13.05	–0.038	0.306	Main Sequence	...	–0.026	–0.003
2MJ06412567+6450318	13.05	–0.063	0.571	AGB	132.599	0.710	–0.048	...	M7
2MJ01493939+6403322	13.06	0.045	0.406	AGB	...	0.129	0.001
2MJ16205657+2121449	13.06	0.035	0.317	Subgiant/giant	39.761	–0.039	–0.005

worldwide and used in this research. This work has made use of the BeSS database, operated at LESIA, Observatoire de Meudon, France: <http://basebe.obspm.fr>.

DATA AVAILABILITY

Table 1 lists the stars discussed in the paper. Their light curves are available from ASAS-SN Sky Patrol v2.0 (Hart et al. 2023).

REFERENCES

- Acerro F., et al., 2015, *ApJS*, **218**, 23
- Addison H., Blagorodnova N., Groot P. J., Erasmus N., Jones D., Mogawana O., 2022, *MNRAS*, **517**, 1884
- Bailer-Jones C. A. L., 2023, *AJ*, **166**, 269
- Baliunas S., Jastrow R., 1990, *Nature*, **348**, 520
- Bellm E., 2014, in Wozniak P. R., Graham M. J., Mahabal A. A., Seaman R., eds, *The Third Hot-wiring the Transient Universe Workshop*. pp 27–33 ([arXiv:1410.8185](https://arxiv.org/abs/1410.8185)), doi:10.48550/arXiv.1410.8185
- Blagorodnova N., et al., 2020, *MNRAS*, **496**, 5503
- Bovy J., Rix H.-W., Green G. M., Schlafly E. F., Finkbeiner D. P., 2016, *ApJ*, **818**, 130
- Boyajian T. S., et al., 2016, *MNRAS*, **457**, 3988
- Chen X., Wang S., Deng L., de Grijs R., Yang M., 2018, *ApJS*, **237**, 28
- Chen X., Wang S., Deng L., de Grijs R., Yang M., Tian H., 2020, *ApJS*, **249**, 18
- Christy C. T., et al., 2023, *MNRAS*, **519**, 5271
- Clements T. D., Henry T. J., Hosey A. D., Jao W.-C., Silverstein M. L., Winters J. G., Dieterich S. B., Riedel A. R., 2017, *AJ*, **154**, 124
- Drimmel R., Cabrera-Lavers A., López-Corredoira M., 2003, *A&A*, **409**, 205
- Duerbeck H. W., et al., 2000, *AJ*, **119**, 2360
- Flesch E. W., 2023, *The Open Journal of Astrophysics*, **6**, 49
- Foukal P., 2017, *ApJ*, **842**, L3
- Gaia Collaboration et al., 2023, *A&A*, **674**, A1
- Gerke J. R., Kochanek C. S., Stanek K. Z., 2015, *MNRAS*, **450**, 3289
- Grankin K. N., Melnikov S. Y., Bouvier J., Herbst W., Shevchenko V. S., 2007, *A&A*, **461**, 183
- Green G. M., Schlafly E., Zucker C., Speagle J. S., Finkbeiner D., 2019, *ApJ*, **887**, 93
- Hambleton K. M., et al., 2023, *PASP*, **135**, 105002
- Hart K., et al., 2023, *arXiv e-prints*, p. [arXiv:2304.03791](https://arxiv.org/abs/2304.03791)
- Heinze A. N., et al., 2018, *AJ*, **156**, 241
- Herbst W., LeDuc K., Hamilton C. M., Winn J. N., Ibrahimov M., Mundt R., Johns-Krull C. M., 2010, *AJ*, **140**, 2025
- Heydari-Malayeri M., 1990, *A&A*, **234**, 233
- Hodgkin S. T., et al., 2021, *A&A*, **652**, A76
- Hosey A. D., Henry T. J., Jao W.-C., Dieterich S. B., Winters J. G., Lurie J. C., Riedel A. R., Subasavage J. P., 2015, *AJ*, **150**, 6
- Hwang H.-C., Zakamska N. L., 2020, *MNRAS*, **493**, 2271
- Iverson R. J., Munari U., Marang F., 1993, *A&A*, **277**, 510
- Jayasinghe T., et al., 2018, *MNRAS*, **477**, 3145
- Jayasinghe T., et al., 2020, *MNRAS*, **491**, 13
- Jayasinghe T., et al., 2021, *MNRAS*, **503**, 200
- Kato T., Ishioka R., Uemura M., 2002, *PASJ*, **54**, 1033
- Kochanek C. S., Beacom J. F., Kistler M. D., Prieto J. L., Stanek K. Z., Thompson T. A., Yüksel H., 2008, *ApJ*, **684**, 1336
- Kochanek C. S., Adams S. M., Belczynski K., 2014, *MNRAS*, **443**, 1319
- Kochanek C. S., et al., 2017, *PASP*, **129**, 104502
- Kozłowski S., et al., 2010, *ApJ*, **708**, 927
- Kraft R. P., 1967, *ApJ*, **150**, 551
- Lomb N. R., 1976, *Ap&SS*, **39**, 447
- Mainzer A., et al., 2014, *ApJ*, **792**, 30
- Marshall D. J., Robin A. C., Reylé C., Schultheis M., Picaud S., 2006, *A&A*, **453**, 635
- Matsumoto T., Metzger B. D., 2022, *ApJ*, **938**, 5
- Metzger B. D., Pejcha O., 2017, *MNRAS*, **471**, 3200
- Metzger B. D., Shen K. J., Stone N., 2017, *MNRAS*, **468**, 4399
- Molnar L. A., et al., 2017, *ApJ*, **840**, 1
- Montet B. T., Simon J. D., 2016, *ApJ*, **830**, L39
- Neiner C., 2018, in Di Matteo P., Billebaud F., Herpin F., Lagarde N., Marquette J. B., Robin A., Venot O., eds, *SF2A-2018: Proceedings of the Annual meeting of the French Society of Astronomy and Astrophysics*. p. Di ([arXiv:1811.05261](https://arxiv.org/abs/1811.05261)), doi:10.48550/arXiv.1811.05261
- Neustadt J. M. M., Kochanek C. S., Stanek K. Z., Basinger C., Jayasinghe T., Garling C. T., Adams S. M., Gerke J., 2021, *MNRAS*, **508**, 516
- Oláh K., Moór A., Kővári Z., Granzert T., Strassmeier K. G., Kriskovics L., Vida K., 2014, *A&A*, **572**, A94
- Paiano S., Landoni M., Falomo R., Treves A., Scarpa R., Righi C., 2017, *ApJ*, **837**, 144
- Paxton B., et al., 2018, *ApJS*, **234**, 34
- Phillips M. J., Hartmann L., 1978, *ApJ*, **224**, 182
- Phillips A., Kochanek C. S., Jayasinghe T., Cao L., Christy C. T., Rowan D. M., Pinsonneault M., 2024, *MNRAS*, **527**, 5588
- Rowan D. M., et al., 2021, *Research Notes of the American Astronomical Society*, **5**, 147
- Scargle J. D., 1982, *ApJ*, **263**, 835
- Shappee B. J., et al., 2014, *ApJ*, **788**, 48
- Shore S. N., Skoda P., Rutsch P., 2013, *The Astronomer’s Telegram*, **5282**, 1
- Simon J. D., Shappee B. J., Pojmański G., Montet B. T., Kochanek C. S., van Saders J., Holoiën T. W. S., Henden A. A., 2018, *ApJ*, **853**, 77
- Smith L. C., et al., 2021, *MNRAS*, **505**, 1992
- Tang S., Grindlay J., Los E., Laycock S., 2010, *ApJ*, **710**, L77
- Teixeira G. D. C., et al., 2018, *A&A*, **619**, A41
- Torres G., Sakano K., 2022, *MNRAS*, **516**, 2514
- Tylenda R., et al., 2011, *A&A*, **528**, A114
- Tzanidakis A., Davenport J. R. A., Bellm E. C., Wang Y., 2023, *ApJ*, **955**, 69
- Warner B., 1995, *Cataclysmic variable stars*. Cambridge Astrophysics Series Vol. 28, Cambridge University Press
- Watson C. L., Henden A. A., Price A., 2006, *Society for Astronomical Sciences Annual Symposium*, **25**, 47
- Weis E. W., 1994, *AJ*, **107**, 1135
- Wenger M., et al., 2000, *A&AS*, **143**, 9
- Winecki D., Kochanek C. S., 2024, *ApJ*, **971**, 61